Development of a discontinuous Galerkin ionosphere-plasmasphere model

Houjun Wang

CIRES, University of Colorado at Boulder

0. Abstract

The objective of this study is to explore the application of high-order numerical methods in ionosphere-plasmasphere modeling (*Wang*, 2022a). Specifically, the nodal discontinuous Galerkin (DG) method is chosen to solve the multifluid dynamical equations along the magnetic field lines. A general curvilinear magnetic field-line-following coordinate system is also used in the model (*Wang*, 2022b). Numerical simulations with different combinations of number of elements (K) and polynomial orders (N) show the *converging* results, indicating the robustness of the algorithms and implementation. The model also captures the dawn terminator effect very well in the He^+ field.

1. Introduction

The high-order methods (formal order of accuracy $p \geqslant 3$) are advantageous for solving the wave propagation problems and/or when more accurate solutions of problems are required (e.g, *Gustafsson*, 2008). High-order spectral methods also have significantly lower phase errors compared to the finite-difference methods (e.g., *Canuto et al.*, 2006). As discussed in *Hesthaven* (2018), the motivation for development of high-order accurate schemes is "to do more with less, i.e., to develop schemes that are more accurate than first order accurate schemes without substantially increasing the computational cost."

The main advantages of the DG methods over classical finite volume and finite difference methods are (*Cockburn et al.*, 2000):

- Arbitrarily high formal order of accuracy can be obtained by suitably choosing the degree of the approximating polynomials
- Highly parallelizable
- Suitable to handle complicated geometries and simple in treating boundary conditions
- Easy in handling adaptivity

2. General curvilinear coordinates

We propose a simple way to define a field-line-following, general curvilinear coordinate system for a general magnetic field:

$$\mu_m = \hat{\Phi}, \quad \chi_m = \frac{\sin^2\theta_m}{r}, \quad \phi_m = \phi_A, \tag{1}$$

where r_A the normalized radial distance to apex, ϕ_A the geographic longitude at apex; $\hat{\Phi}$ the normalized magnetic potential (by dipole moment g_m), θ_m the magnetic colatitude defined by

$$\frac{\sin^2\theta_m}{r} = \frac{1}{r_A}. \tag{2}$$

And the conventional covariant-contravariant formalism is used throughout. Other features include:

- It reduces to a dipole coordinate system when the magnetic field is a pure dipole.
- Highly accurate results are obtained using the high-order ODE solver to solve the general magnetic field line equations.
- Numerical results show that this general curvilinear coordinate system is also an Euler potential or Clebsch-type coordinate system.
- The general coordinate system is used in the development of discontinuous Galerkin (DG) ionospheric model.

3. Overview of the DG model

Using the operator splitting, the advection-diffusion-chemical ($\mathcal{ADC}$) operators are treated sequentially as follows:

$$\frac{\partial q}{\partial t} = \mathcal{C}(\delta t)\mathcal{D}(\delta t)\mathcal{A}(\delta t)q, \tag{3}$$

- The advection ($\mathcal{A}$) and diffusion ($\mathcal{D}$) are solved using the high-order nodal DG methods.
- The physical-chemical forcing ($\mathcal{C}$) is added using a positive-definite ODE solver.
- Simple perpendicular ExB transport is solved using the traditional semi-Lagrangian (SL) scheme.
- The model uses the ragged array of variable length to better handle the varying number of points along different field lines. It also uses the MPI-IO for efficient parallel I/O.

4. The DG for field-aligned dynamics

Write the set of equations in the vector form as

$$\frac{\partial \boldsymbol{q}}{\partial t} + \frac{\partial \boldsymbol{F}}{\partial x} = \boldsymbol{G}, \tag{4}$$

where

$$\boldsymbol{q} = \begin{bmatrix} \rho_i \\ \rho_i u_i \\ E_i \end{bmatrix}, \quad \boldsymbol{F} = \begin{bmatrix} h_\chi h_\phi(\rho_i u_i) \\ h_\chi h_\phi(p_i + \rho_i u_i^2) \\ h_\chi h_\phi(E_i + p_i)u_i \end{bmatrix}, \quad \boldsymbol{G} = \begin{bmatrix} 0 \\ -\rho_i g_{\shortparallel} \\ -\rho_i u_i g_{\shortparallel} \end{bmatrix}.$$

Let

$$\boldsymbol{q}_h^k(x,t) = \sum_{i=1}^{N_p} \boldsymbol{q}_h^k(x_i^k,t)\ell_i^k(x), \quad \boldsymbol{F}_h^k(\boldsymbol{q}_h^k(x,t)) = \sum_{i=1}^{N_p} \boldsymbol{F}_h^k(x_i^k,t)\ell_i^k(x),$$

We have

$$\int_{\mathsf{D}^k}\left(\frac{\partial \boldsymbol{q}_h^k}{\partial t} + \frac{\partial \boldsymbol{F}_h^k}{\partial x} - \boldsymbol{G}_h^k\right)\ell_j^k(x)dx = 0. \tag{5}$$

$$\int_{\mathsf{D}^k}\left(\frac{\partial \boldsymbol{q}_h^k}{\partial t}\ell_j^k - \boldsymbol{F}_h^k\frac{d\ell_j^k}{dx} - \boldsymbol{G}_h^k\ell_j^k\right)dx = -[\boldsymbol{F}_h^k\ell_j^k]_{x_l^k}^{x_r^k}. \tag{6}$$

$$\int_{\mathsf{D}^k}\left(\frac{\partial \boldsymbol{q}_h^k}{\partial t}\ell_j^k - \boldsymbol{F}_h^k\frac{d\ell_j^k}{dx} - \boldsymbol{G}_h^k\ell_j^k\right)dx = -[\boldsymbol{F}^*\ell_j^k]_{x_l^k}^{x_r^k}. \tag{7}$$

Integration by parts once more, we get the DG scheme in *strong form* as

$$\int_{\mathsf{D}^k}\left(\frac{\partial \boldsymbol{q}_h^k}{\partial t} + \frac{\partial \boldsymbol{F}_h^k}{\partial x} - \boldsymbol{G}_h^k\right)\ell_j^k(x)dx = [(\boldsymbol{F}_h^k - \boldsymbol{F}^*)\ell_j^k]_{x_l^k}^{x_r^k}. \tag{8}$$

In matrix form this can be written as

$$\mathcal{M}^k\frac{d}{dt}\boldsymbol{q}_h^k + \mathcal{S}\,\boldsymbol{F}_h^k - \mathcal{M}^k\boldsymbol{G}_h^k = \left[\boldsymbol{\ell}^k(x)(\boldsymbol{F}_h^k - \boldsymbol{F}^*)\right]_{x_l^k}^{x_r^k}, \tag{9}$$

where we have introduced the local mass and stiffness matrices

$$\mathcal{M}_{ij}^k = \int_{\mathsf{D}^k}\ell_i^k(x)\ell_j^k(x)dx, \quad \mathcal{S}_{ij}^k = \int_{\mathsf{D}^k}\ell_i^k(x)\frac{d\ell_j^k}{dx}dx. \tag{10}$$

More details on model numerics and numerical experiments can be found in *Wang* (2022a).

5. Total electron contents (TEC)

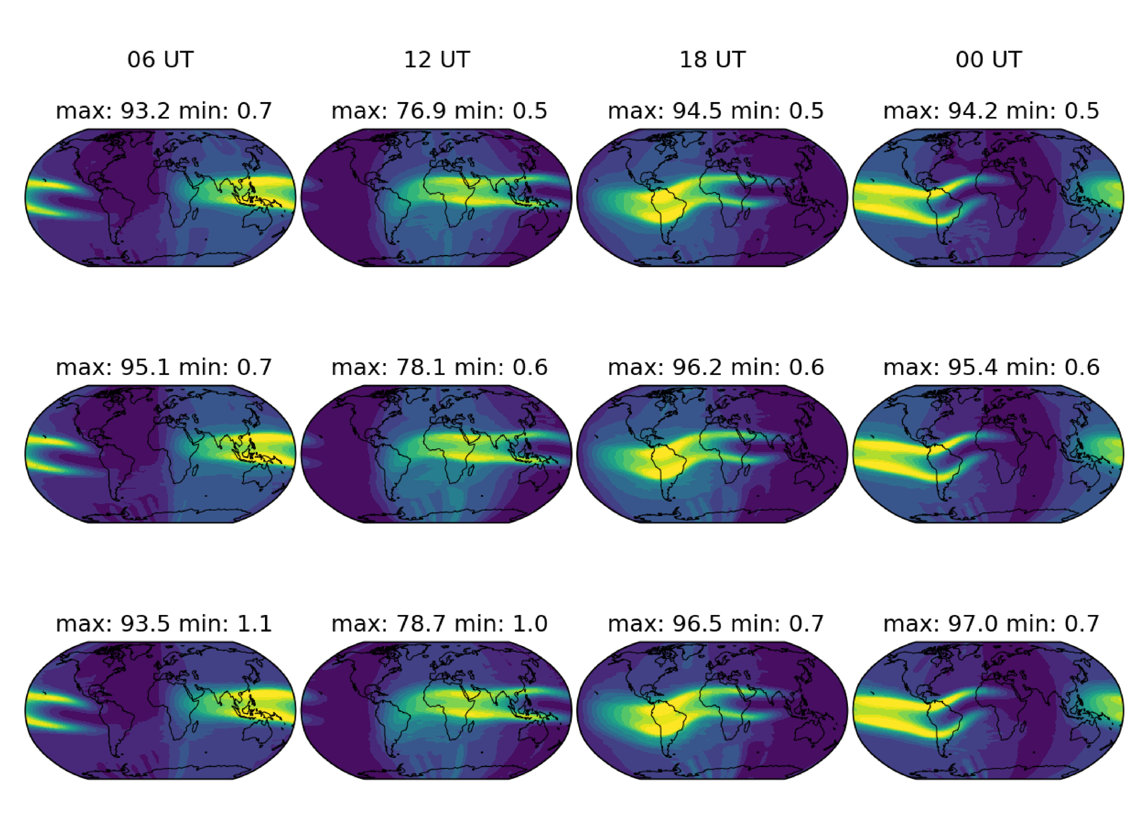

Figure 1: TEC simulations, using the same number of elements (K101), but varying polynomial orders N: the first row is with N2, the second row with N3, and the third row with N4. Four UT times (06, 12, 18, and 00 UT) are shown, respectively for 6, 12, 18 and 24 hour simulations, initialized at 00 UT on 21 March 2000.

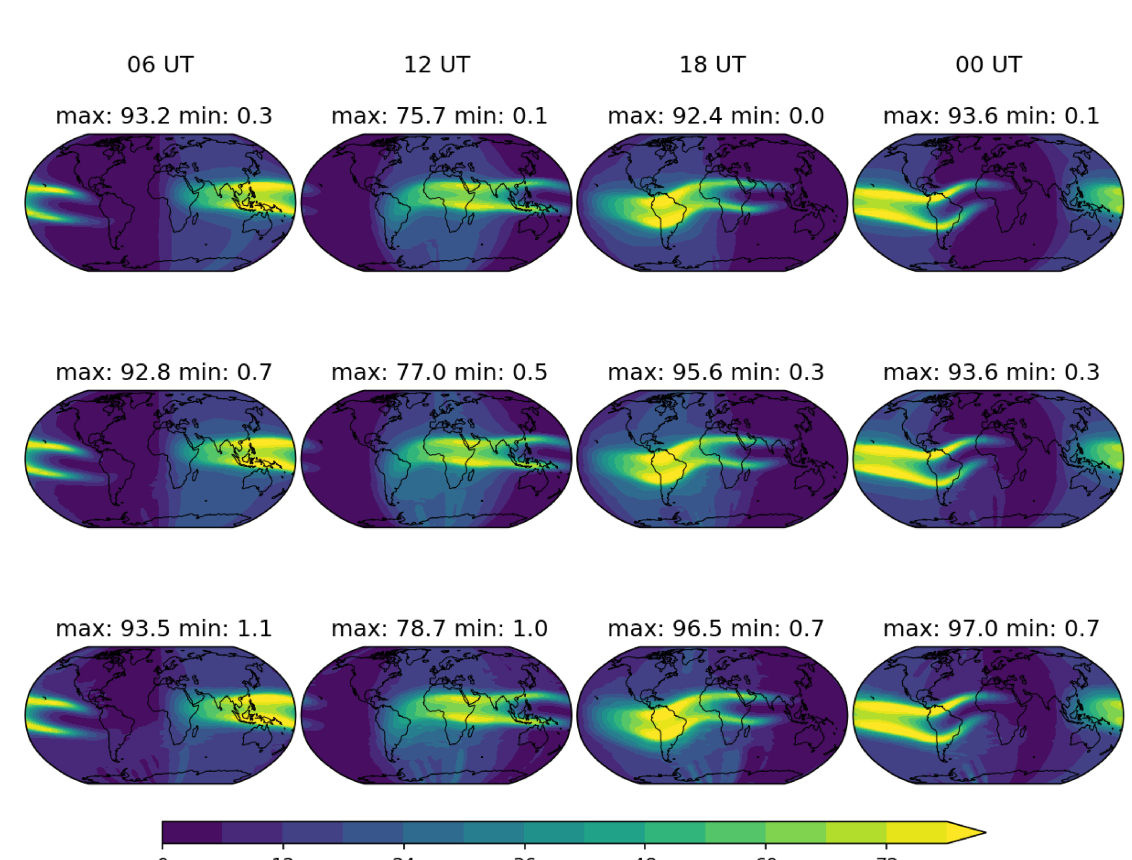

Figure 2: TEC simulations, using varying number of elements K and varying polynomial orders N: the first row is with K201 and N2, the second row with K135 and N3, and the third row with K101 and N4. Four UT times (06, 12, 18, and 00 UT) are shown, respectively for 6, 12, 18 and 24 hour simulations, initialized at 00 UT on 21 March 2000.

6. Capture the terminal effect

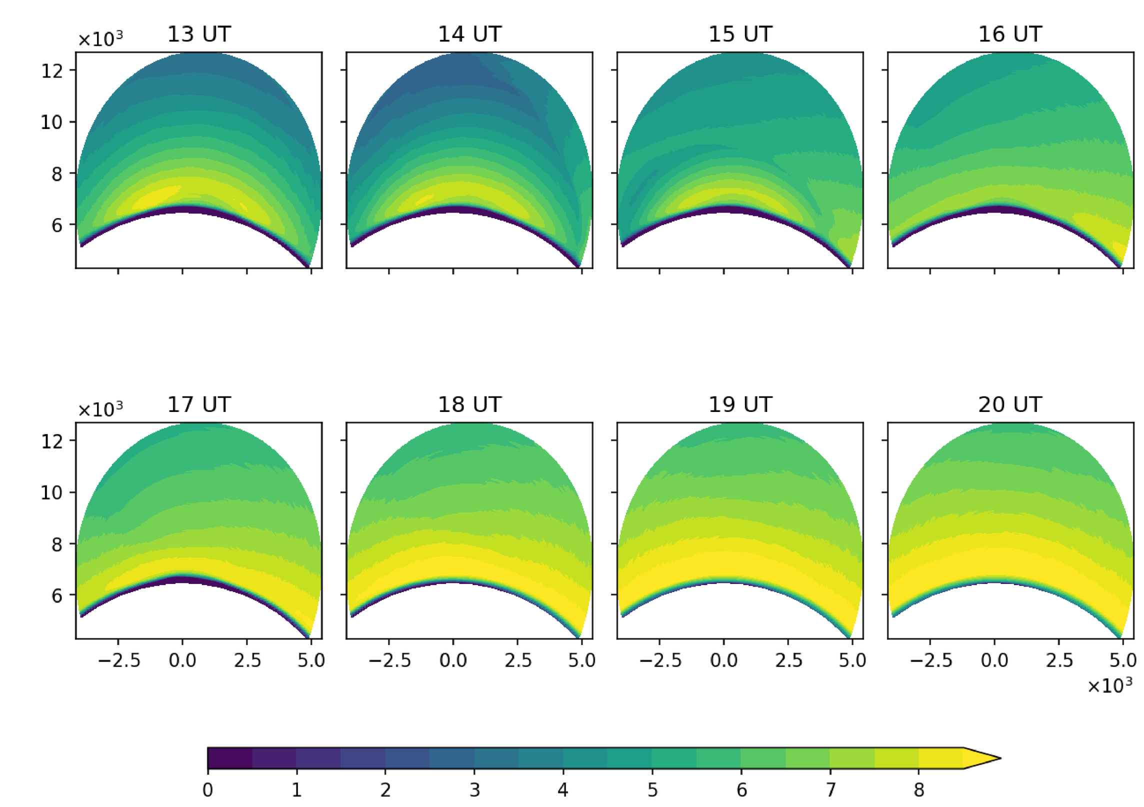

Figure 3: The meridional plane plot of the He^+ density, $\log_{10} n_{He^+}$ [m^{-3}], at the magnetic longitude 180°, showing the dawn terminator effect. The simulation results from the K101/N2 run are shown every hour from 13 to 20 UT, initialized at 00 UT on 21 March 2000. The geocentric x- and y-coordinates in [10^3 km] are used in the plot, with x from north to south.

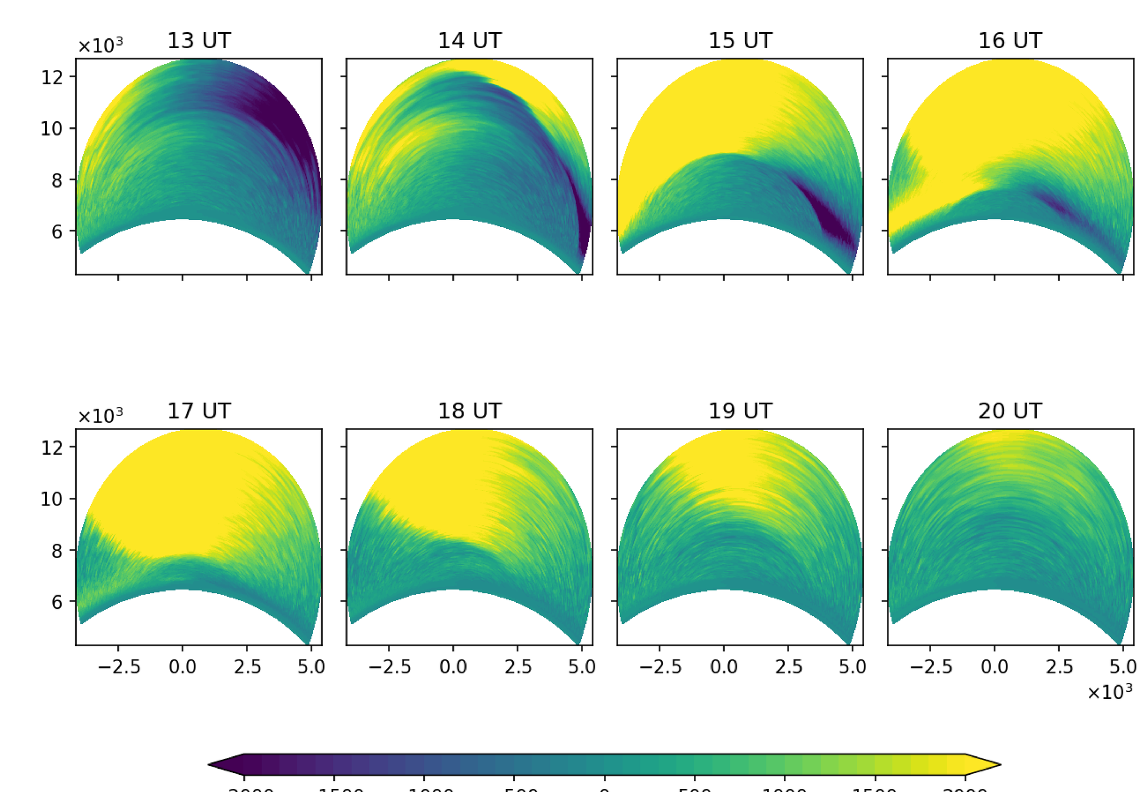

Figure 4: Same as Fig. 3, but for He^+ velocity [$m\,s^{-1}$] along the field line.

7. Summary

- The high-order discontinuous Galerkin (DG) method is used to solve the multifluid plasma dynamical equations (conservation laws with gravity and thermal diffusion) along the magnetic field line.
- A positive-definite integration scheme, the Patankar-Euler scheme, is used to solve the physical-chemical ODEs.
- The model uses the ragged array of variable length to better handle the varying number of points along different field lines. It also uses the MPI-IO for efficient parallel I/O.
- Simple specified ExB drift velocities and semi-Lagrangian transport scheme are used for the perpendicular dynamics.
- Converging results of simulations with different element size and polynomial order indicate robustness of algorithms and implementation.
- The model algorithms also capture the dawn terminator effect very well in the He^+ density and wind fields.

8. Future work

- DG solver for ionospheric electrodynamic equation
- DG scheme for ExB transport
- DG solver for photoelectron heating
- Extend to high latitudes

9. References

Wang, H. (2022a), Development of a discontinuous Galerkin ionosphere-plasmasphere model, *J. Geophys. Res. Sp. Phys.*, p. 19, doi:10.1029/2021JA030047.

Wang, H. (2022b), A general curvilinear magnetic field-line-following coordinate system for ionosphere-plasmasphere modeling, *J. Geophys. Res. Sp. Phys.*, p. 13, doi:10.1029/2021JA030017.